

A techno-economic analysis of PV solar modules attached to vertical facades of a residential building in a hot arid climate

Hamad H. Almutairi*, Ali F. Alajmi*^{***} and Nabil A. Ahmed**

* Mechanical Engineering Department, College of Technological Studies, PAAET, Kuwait.

** Electrical Engineering Department, College of Technological Studies, PAAET, Kuwait.

*** Corresponding Author: af.alajmi@paaet.edu.kw

Submitted : 12/11/2021

Revised : 08/01/2022

Accepted : 19/01/2022

ABSTRACT

This paper investigates the feasibility of electrical power generation using differently orientated photovoltaic (PV) modules attached to vertical surfaces. The global horizontal irradiance (GHI) has been measured to verify the commonly used corresponding mathematical models. However, the solar irradiances on vertical surfaces are calculated concerning directional orientation using recently validated mathematical models of similar climates. A selected case representing the predominant construction style for houses in Kuwait was used to examine the PV configuration proposed on the house's façade at different promising orientations, east, west, and south. The total generated electrical power from the three promising façades (100 MW) is almost twice the roof's amount (57 MW). A detailed economic evaluation using lifecycle cost analysis (LCC) was conducted through a 25-year plan. It includes a suggested investment plan for the annual cash resulting from avoided conventional electrical power. Promisingly, the economic analysis proved that the vertical façades east, west, and south are feasible at payback years of around 8, 8, and 15, respectively, while the rooftop PV has the best economic feasibility by a payback period of 5 years. The outcome encourages policymakers to incentivize the vertical surfaces to harvest solar energy, particularly with the expectation of a further decline in PV prices.

Keywords: Vertical solar irradiance; Photovoltaic (PV); Electrical power generation; Lifecycle cost analysis (LCC); Building attached photovoltaic (BAPV).

INTRODUCTION

Buildings account for about 40% of global energy consumption and about 30% of global greenhouse gas emissions [Nejat, P. et al., 2015]. A large amount of the energy use is due to the increasing demands on cooling and heating applications [Yang, L. et al., 2014]. The need to consider effective solutions related to the enormous current and future energy demand by buildings is necessary. It should be highly evident that adding new capacity to electricity grids is not a sustainable solution if the installed power capacity uses the same conventional power generation technologies, since most of the power plants use nonrenewable energy resources.

The urge to adopt renewable energy resources to sustain that rapid demand for electricity is vital. Renewable power capacity is expected to grow by 50% between the years 2019 and 2024, headed by PV solar energy [IEA renewables, 2019]. The total global installed capacity of PV crossed 600 GW in 2019; from this amount, China is a notable example of the largest market for PV solar in the world, with a total installed capacity of 204.7 GW [IEA PVPS, 2020].

The decision to involve PV energy into the building's envelope has received significant attention due to the decrease in the cost of solar cells. The application of this involvement is classified as building applied PV (BAPV) system and building integrated PV (BIPV) [Karthick, A. et al., 2017]. The potential of generating electrical power from vertical facades is a topic of high interest. Building integrated PV (BIPV) could be a leading technology with regards to cost and efficiency [Lee, M. et al., 2017]. In the same study, the authors indicated that BIPV system efficiency is influenced by other factors such as shading effects and the directional orientation. Vertically installed PV on facades, in certain latitudes, receives less solar irradiance compared to the roof, particularly in summer, but can produce relatively more electrical energy during winter [Hsieh, M. et al., 2013]. Installing PV modules on vertical façades for a building with more than one façade can help harvest solar energy at different times of the day [Hummon, M. et al., 2013]. From the architectural point of view, installing PV on the building envelope can replace the conventional cladding materials [Montoro, F. et al., 2011].

The short amount of measured solar energy irradiance on vertical surfaces is a considerable limitation to examining PV technology on vertical surfaces in many places. However, efforts to measure solar radiation incidents on tilted surfaces have been recorded at a few locations [Muneer, T., 1990; University of Oregon, 2020; Şaylan, L. et al., 2002; Notton, G. et al., 2006; Li, W. et al., 2002]. Furthermore, several studies have focused on calculating solar irradiances for tilted surfaces [Cucumo, M. et al., 2007; Loutzenhiser, G. et al., 2007]. The accurate calculation of the tilted diffuse solar irradiance is what distinguishes models from each other. Moreover, the essential criterion for selecting the most suitable model for simulating the electrical output of a PV module is its ability to simulate the diffuse radiation of the sky under all weather conditions. From this perspective, Mubark et al. [Mubarak, R. et al., 2017] examined different models that are widely used in the literature [Liu, B. and Jordan, R., 1961; Hay, E. and Davies, A., 1978; Reindel, T. et al., 1990; Perez, R. et al., 1990]. They found that the best models that have been examined are Hay and Davies for east and west orientations and Preze model for north and south orientations.

This work aims to evaluate the financial benefits of installing PV solar modules on vertical facades for a typical house in a hot arid climate, Kuwait. The PVs' expected generated power is predicted based on verified global horizontal irradiance model against measured data. Then, two mathematical models were used to calculate vertical solar irradiances at east, west, and south directional orientations based on the models [Perez, R. et al., 1990] for south orientation and [Hay, E. and Davies, A., 1978] for east and west directional orientations. The study presents an economic evaluation for the installed PV using Lifecycle Cost Analysis. It also illustrates an economical approach to utilizing the cash savings from avoided conventional electrical power. The novelty of this work is establishing monthly vertical solar irradiances data, in addition to following an economic approach on how to shorten the payback period of vertical PV installations.

SOLAR IRRADIANCE MATHEMATICAL MODELS

Basic Solar Components

The amount of solar radiation on the horizontal surface at any location on the surface of the earth can be calculated as a fraction of the amount of that incident outside the earth's using the following Equations [Khalil A., Shaffie M., 2013].

$$I_0 = \left(\frac{24}{\pi}\right) I_{SC} E_o [\cos\varphi \cos\delta \sin\omega + (\pi\omega/180) \sin\varphi \sin\delta] \quad (1)$$

$$E_o = 1 + 0.033\cos(2\pi d_n/365), \quad (2)$$

$$\omega = \cos^{-1}(-\tan\varphi \tan\delta), \quad (3)$$

$$\delta = 23.45 \sin\left\{\frac{360(n+284)}{365}\right\} \quad (4)$$

where I_{SC} is the average extraterrestrial solar irradiance, which is 1361.1 W/m^2 , E_o is the correction factor of earth's orbit, ω is hour angle, d_n is the day of the year, φ is the latitude, and δ is the solar declination angle of the sun [Spencer W., 1975].

Global Horizontal Irradiance Models

There are many experimental and theoretical models for calculating different tilts and orientations. These models are tested to find the best fit of the area under study. Global horizontal irradiance models are a sum of the horizontal beam and diffuse radiations as

$$I_H = I_{h,d} + I_{h,b} \quad (5)$$

where $I_{h,d}$ is diffuse and $I_{h,b}$ is the horizontal beam radiations. The measurement of diffused radiation requires costly equipment and sustained high maintenance. For this reason, several mathematical models have been defined to estimate diffuse radiation on horizontal surfaces; decomposition models have been proved to be more accurate [Mousavi Maleki, A. et al., 2017]. Decomposition models are based on a correlation between the diffuse and total radiation on a horizontal surface. This correlation is defined as a clearness index that varies according to time of the year, season, climatic conditions, and geographical situation of a place [Kumar, R., 2005 and Umanand, L. et al., 2015].

$$M_t = \frac{I_H}{I_o} \quad (6)$$

where M_t is the clearness index. An hourly clearness index derived for Kuwait from a local data represented by mixture distributions model is used in this study [Tye, R., et al., 2019].

There is no universal model that could be conclusively used; in this study, many decompositions diffused models have been tested against the global horizontal measured data, and the best agreement was with Reindel et al. [Reindel, T. et al., 1990] with the following formulas:

$$\begin{aligned} 0 < M_t \leq 0.3 & \quad I_d = (1.02 - 0.254M_t + 0.0123\sin\alpha) I_H \\ 0.3 < M_t \leq 0.78 & \quad I_d = (1.4 - 1.749M_t + 0.177\sin\alpha) I_H \\ 0.78 < M_t \leq 1 & \quad I_d = (0.486M_t + 0.182\sin\alpha) I_H \end{aligned} \quad (7)$$

where α is the solar elevation. Then, the direct radiation can be estimated using the following equation:

$$I_{h,b} = I_H - I_{h,d} \quad (8)$$

Then, the direct normal radiation I_{bN} also can be found from the following equation:

$$I_{h,b} = I_{bN} \cos \theta_z \quad (9)$$

where θ_z is the zenith between the beam from the sun and vertical angle and expressed as

$$\cos \theta_z = \sin \delta \sin \varphi + \cos \delta \cos \varphi \cos \omega \quad (10)$$

Validating the Measured Global Horizontal Data

The experimental data for this study were gathered at a facility located on the roof of a public building near the Kuwait City (29°N; 48°E; 56m above mean sea level). The experimental data averages of global horizontal radiation (GHR) were recorded every 5 min. Cumulative hourly, daily, and monthly values were calculated from the average of hourly data. The measured global horizontal data for four different seasonal days were compared to the ones found from the best mathematical models; see Fig 1. As shown in Fig. 1, the trend between measured and modeled is in a good agreement on an hourly basis of the tested days. The only noticeable deviation can be seen on December 21. The cause of deviation can be justified as the day may be a cloudy or dusty weather day. Dusty weather leads to fast changes in the solar insolation and may lead to nonuniform distribution or partial shading conditions of the solar insolation on the surface of PV panel [Ahmed, N. et al., 2022, Jallal, M., et al., 2021]. In contrast to the hourly data, the average daily and monthly data of the solar irradiance show good agreement with the mathematical model, Reindal, and the deviation is less than 10% as shown in Figure 2. Also, Figure 2, coincident with experienced high solar irradiance, occurs in the middle of summer season during the months of June and July.

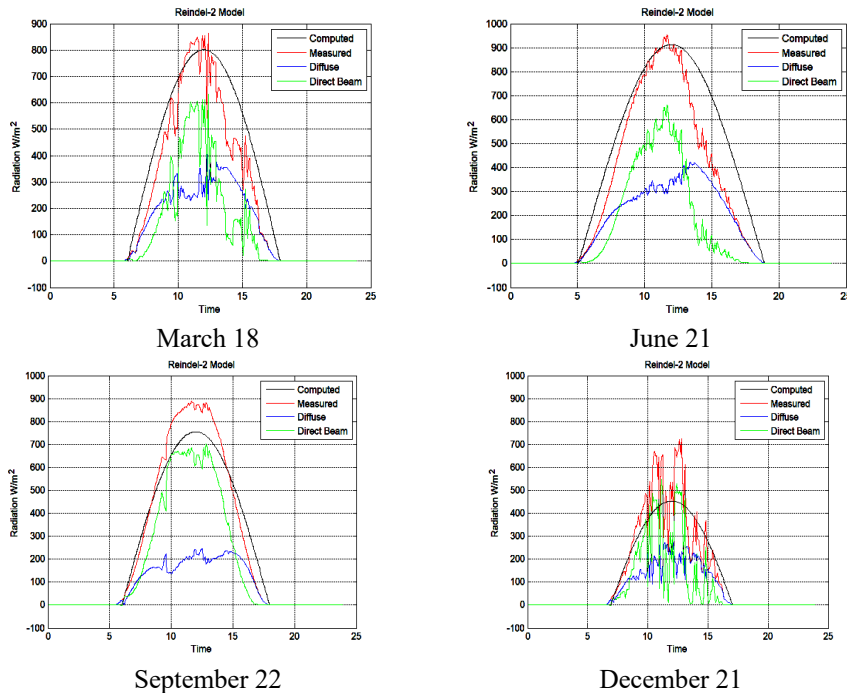


Figure 1. Comparison between the measured horizontal data and Reindal model.

Estimating Vertical Surfaces Irradiance

Measured horizontal irradiance components (global, diffuse, and direct) constitute the most important input data to compute the tilted irradiance (I_T). Modeling of I_T would be ideal if the measurements of all irradiance components, including ground reflectance, are available, which require costly equipment and sustained maintenance. However, it is expressed to be as follows:

$$I_T = I_{t,b} + I_{t,d} + I_g \tag{11}$$

where $I_{t,b}$ is the beam tilted, $I_{t,d}$ is the sky diffuse tilted, and I_g is the ground reflected.

Estimating Direct Beam Radiation on Vertical Surfaces

Direct beam radiation value on an angled surface can be calculated using the following Equation:

$$I_{t,b} = r_b I_{h,b} \tag{12}$$

where r_b is the ratio of hourly radiation received by an angled surface to that of a horizontal surface outside the earth’s atmosphere.

$$r_b = \frac{I_{o\beta}}{I_o} \approx \frac{\cos\theta_0}{\cos\theta_z} \tag{13}$$

where θ_0 is the angle between insolation and surface normal, for a surface inclined in any arbitrary direction; and θ_z is the zenith angle, or the angle between the beam from the sun and vertical surface:

$$\cos\theta_0 = \sin\delta \sin(\varphi - \beta) + \cos\delta \cos(\varphi - \beta) \cos\omega \tag{14}$$

where β is the inclined surface angle.

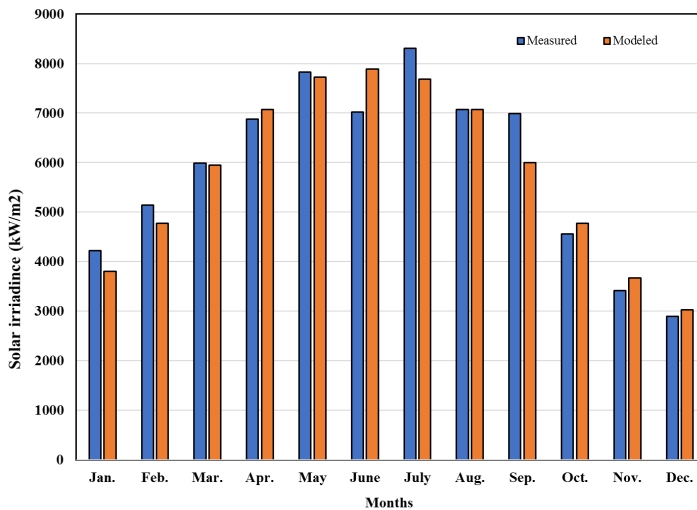


Figure 2. Monthly solar irradiance comparison between measured and modeled.

Estimating Diffused Radiation on Vertical Surfaces

Inaccurate calculations of diffuse irradiance can lead to an unprecise estimation in the annual energy yield of a PV system by as much as 8% [Hofmann, M. and Seckmeyer, G., 2017]. The influence of albedo value on the calculated tilted irradiance increases as the tilt angle increases. There are many models that can be used to compute the diffuse part of Equation (10). The best models that have been found on literature that have similar climate are Hay and Davies for east and west orientations and Preze model for north and south orientations [Mubarak, R. et al., 2017].

East and West Orientations Model

The Hay and Davies diffuse model divides the sky's diffuse irradiance into isotropic and circumsolar components only. The horizon brightening was not considered:

$$I_{t,d} = (I_{h,b} + I_{h,d}A)r_b + I_{h,d}(1 - A) \left(\frac{1 + \cos \beta}{2} \right) + I_{hp} \left(\frac{1 - \cos \beta}{2} \right) \quad (16)$$

$$A = \frac{I_{bn}}{I_{on}} \quad (17)$$

where $I_{h,b}$ and $I_{h,d}$ are the hourly direct beam and diffuse insolation incident on a horizontal surface, respectively. A represents the transmittance of beam irradiance through the atmosphere, where I_{bn} is the direct-normal solar irradiance, and I_{on} is the direct extraterrestrial normal irradiance.

North and South Orientations Model

Perez model represents a more detailed analysis of the sky diffuse radiation. The model divided the diffuse irradiances into three components of isotropic background, circumsolar brightening, and horizon brightening [Perez, R. et al., 1990], as shown in the following equation:

$$I_{t,d} = I_{h,d} \left[(1 - F_1) \left(\frac{1 + \cos \beta}{2} \right) + F_1 \frac{a}{b} + F_2 \sin \beta \right] \quad (18)$$

where F_1 and F_2 are circumsolar and horizon brightness coefficients, respectively; a and b are solid angles corresponding to the circumsolar part and can be computed as

$$a = \max(0, \cos \theta) \quad (19)$$

$$b = \max(\cos 85^\circ, \cos \theta_z) \quad (20)$$

F_1 and F_2 in Equation (17) are functions of clearness \mathcal{E} , zenith angle Θ , and brightness Δ . These factors are defined as

$$\mathcal{E} = \frac{I_d + I_b + 5.535 \times 10^{-6} \theta_z^3}{I_d + 5.535 \times 10^{-6} \theta_z^3} \quad (21)$$

$$\Delta = m \frac{I_d}{I_o} = \frac{1}{\cos \theta_z} \frac{I_d}{I_o} \quad (22)$$

The coefficients F_1 and F_2 are then computed as

$$F_1 = \max \left[0, \left(f_{11} + f_{12}\Delta + \frac{\pi\theta_z}{180} f_{13} \right) \right] \quad (23)$$

$$F_2 = f_{21} + f_{22}\Delta + \frac{\pi\theta_z}{180} f_{23} \quad (24)$$

The coefficients f_{11} , f_{12} , f_{13} , f_{21} , f_{22} , and f_{23} are the clearance coefficients of experimental data for similar locations [Perez, R. et al., 1990].

Estimating Ground-Reflected Radiation on Vertical Surfaces

The hourly ground-reflected radiation by the earth's surface can be calculated as

$$I_r = I_H \rho \left(\frac{1 - \cos \beta}{2} \right) \quad (25)$$

where ρ is the ground albedo estimated at a constant value of 0.2 [Gueymard, A., 2009].

STUDIED RESIDENTIAL BUILDING

Description of the Studied Residential Building

The studied residential building model represents the predominant construction style preferred by families in Kuwait. There is a three-storey house with uniform geometry and rectangular shape facades; see Figure 3. The methodology of installing PV modules is to distribute PV modules on the facade excluding the area allocated for windows, and on the roof as a benchmark. The performance of vertical facade's PV modules is to be examined at three directional orientations (South, East, and West). More details about the building's geometries are given in Table 1.



Figure 3. (a) Isotropic view of the building model (b) geometry of vertical facade proposed for PV analysis.

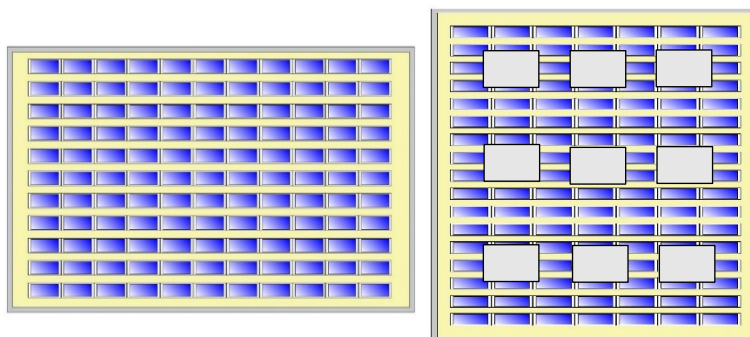
PV Modules Installation

The PV modules entirely cover the facades except the windows and uniformly distributed; the windows area occupies 30% of the façade area based on the standard specifications for construction and buildings, Public Authority for Housing Welfare. For the roof's installation, the distribution of modules does not cover the whole roof's area. This is for the considerations of installation of air conditioner units, maintenance, and movements and to avoid shading effects.

The selected PV module type is the SI-mono model CS3U-380MS, which has a nameplate capacity of 380 Watt [Abdulrahman, A., 2020]. The CS3U-380MS model is a high efficiency and high-power PV classes for equivalent module sizes. It has the following advantages: high module efficiency up to 19.15%, low hot spot temperature risk, low temperature coefficient $-0.37\%/^{\circ}\text{C}$, and high NMOT (Normal Module Operating Temperature) of $42 \pm 2\text{ }^{\circ}\text{C}$. Configurations of PV modules in each installation's area are indicated in Table 3.

Table 1. Characteristics of the building's geometries.

Parameter	Details
Plan shape	Rectangular
Number of stories	3
Roof area	400 m ²
Floor-to-floor height	4 m
Small Façade area	192 m ²
Windows area	30% of the façade area,



(a) Roof area

(b) façade excluding windows area

Figure 4. Distribution of PV modules (a) roof (b) vertical façade.

Table 3. Configurations of PV modules in each installation area.

Installation	Modules Area (m ²)	Cells Area (m ²)	Arrangement of PV Modules
Roof	119	106	<ul style="list-style-type: none"> • In series= 15 modules • In parallel= 4 strings • Total = 60 modules • Tilt angle =27° facing south
Vertical Facade	135	120	<ul style="list-style-type: none"> • In series= 17 modules • In parallel= 4 strings • Total = 68 modules • Tilt angle = 90 ° facing east, south, west

The performance of PV modules configured horizontally on the roof and vertically on facades at different orientations is based on the average monthly solar irradiance of Wh/m². Thus, the electrical power generated (E_{mod}) can be calculated by multiplying the gained solar power (Q_s) with the total cells area (A_{cell}), also considering an efficiency factor (η_m) of 19.1% and inverter efficiency ($\eta_{inverter}$) of 98.1%, as shown in equation (26) [Hsieh, M., et al., 2013].

$$E_{mod} = Q_s \times \eta_{module} \times A_{Cell} \times \eta_{inverter} \quad (26)$$

OVERVIEW ECONOMIC ANALYSIS

Lifecycle Cost Analysis (LCCA)

The calculation of life-cycle cost requires that all costs be identified by year during the lifespan of the modules. PV modules commonly come with 25 years warranty with annual average degradation of 0.85% each year. It considers the costs that would be paid during the studied period, which includes the installation cost of the PV system (Capital Cost), and operation and maintenance (O&M) cost of the installed PV system, according to the following expression:

$$C = \text{Installation} + (\text{Operation \& Maintenance}) \quad (27)$$

The installation cost for the selected module type (mono-SI-380 W) for the studied configurations is USD 1000/kWp for the roof's configuration and USD 1400/kWp for the vertical configuration on the façade. The difference in installation prices herein is explained by the special materials needed for fixation in vertical facades, in addition to the higher labor cost and special equipment for working at height, while the annual operation and maintenance costs are estimated to be around USD 50/kWp [Abdulrahman, A., 2020]. Life-cycle cost analysis involves rational calculations. The work considered the "present-value method" (P_v) to estimate the life-cycle cost in the present value. P_v calculations depend on the time equivalent value of past, present, or future cash flows as of the beginning of the base year [Mohammad, A., et al., 2021, Shwehdi, M., et al., 2015, Abotalib Fuller, S. and Petersen, S., 1995]. It considers all expenses that are presented in equation (27) using equation (28). The Uniform Present Value (UP_v) factor is used to calculate the P_v of a series of cash amounts (C) that are paid over a period of (n) years.

$$P_v = C \times UP_v \quad (28)$$

UP_v represents the uniform present-worth factor, which can be calculated using the following equation (29) [Fuller, S., and Petersen, S., 1995]:

$$UP_v = \left[\frac{(1+d)^n - 1}{d(1+d)^n} \right] \quad (29)$$

A uniform discount rate (d) is applied to the cash flow to calculate the net present value. The discount rate is a function of interest rate (i) and inflation rate (j) as shown in equation (30) [Fuller, S., and Petersen, S., 1995]:

$$d = \frac{i - j}{1 + j} \quad (30)$$

According to the latest financial statistics in Kuwait, it was found that there was an average interest rate of 3 %, while inflation was 2 % based on the increase in the consumer price index between the two financial years (2018-2019) [Central Bank of Kuwait, 2019]. Thus, to calculate the LCCA from equation (27), the operations and maintenance cost is multiplied by the uniform present value factor (UP_v) because it is expected to escalate in the future because of the rise in workers' wages and other elements included in the annual O&M costs.

Investment Plan For The Saved Cash

The avoided conventional electrical power (E_{av}) is the net electrical power, which equals the difference between what the PV modules generate (E_{mod}) and the annual degradation (E_{Deg}). The explanation for this is that the building needs to compensate what is annually lost due to the PV system's degradation. Equation (31) shows how avoided electrical power is calculated.

$$E_{Av} = E_{mod} - E_{Deg} \quad (31)$$

Therefore, equation (32) represents the annual cost of avoided conventional electrical power (CA). The production cost of conventional electrical power plants (Pro_{con}) in Kuwait is estimated to be U.S.\$ 0.133 /kWh [Ministry of electricity and water (MEW), 2019].

$$CA = E_{Av} \times pro_{con} \quad (32)$$

The cost that was avoided represents the future value that is saved (FV); so, it is subjected to be invested at a compounding interest rate (i) during the study period (n). Equation (33) represents the total future savings resulting from avoided conventional power cost (CA):

$$FV = CA_n(1+i)^{n-n} + CA_{n-1}(1+i)^{n-(n-1)} + \dots + CA_1(1+i)^{n-1} \quad (33)$$

Return on Investment

The return on investment (ROI) for the installed PV system is calculated based on the ratio between the net profit and the total invested cost. The net profit was calculated as the annual returns from the avoided conventional electrical power represented in equation (33), while the total invested cost was represented as total cash paid through

the lifecycle represented in equation (27). Therefore, the return on investment can be calculated as shown in the following equation:

$$ROI = \frac{FV}{LCC} * 100 \tag{34}$$

RESULTS AND DISCUSSION

Computed Vertical Irradiances

As shown in Figure 5, it is noticeable that the north vertical irradiances barely appear at minimum values during summer months, the reason why we neglect this orientation from the analysis. But, for the other directional orientations, the west and east façades show a significant superiority compared to south façade most of the year except winter and fall seasons during months of November, December, January, and February. This distribution of irradiance on the vertical facades can be justified as a result of geographical location of Kuwait City.

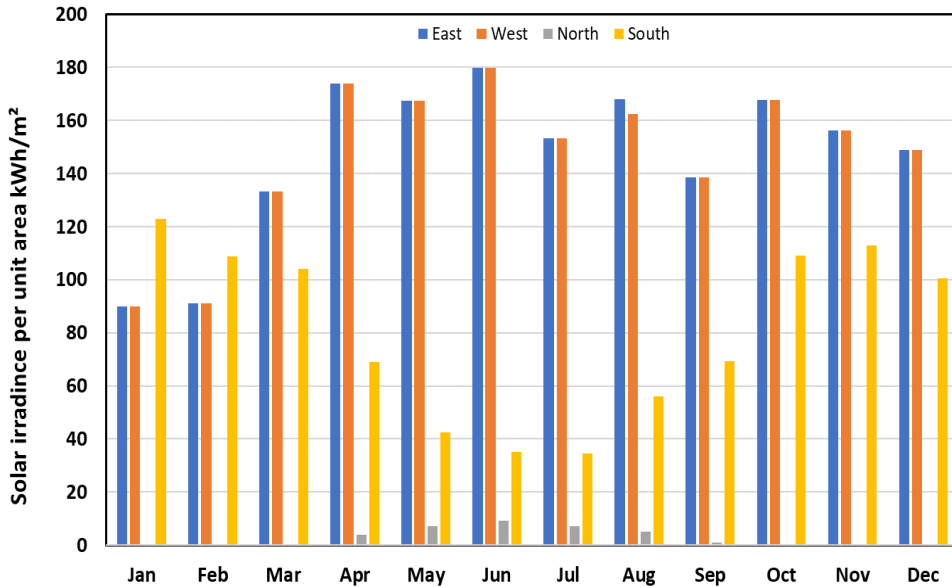


Figure 5. Calculated monthly global vertical irradiance at different directional orientation.

PV Modules Electricity Generation

The selected case study was used to make a quantitative analysis of the intended performance and economic evaluation. Using the characteristics and details related to the selected PV module, the PV electrical power generation capabilities for the studied installation configurations were calculated. It was found that the roof and the facade generate electricity similar to the trend that was found in solar energy harvesting behavior, as shown in Figure 6.

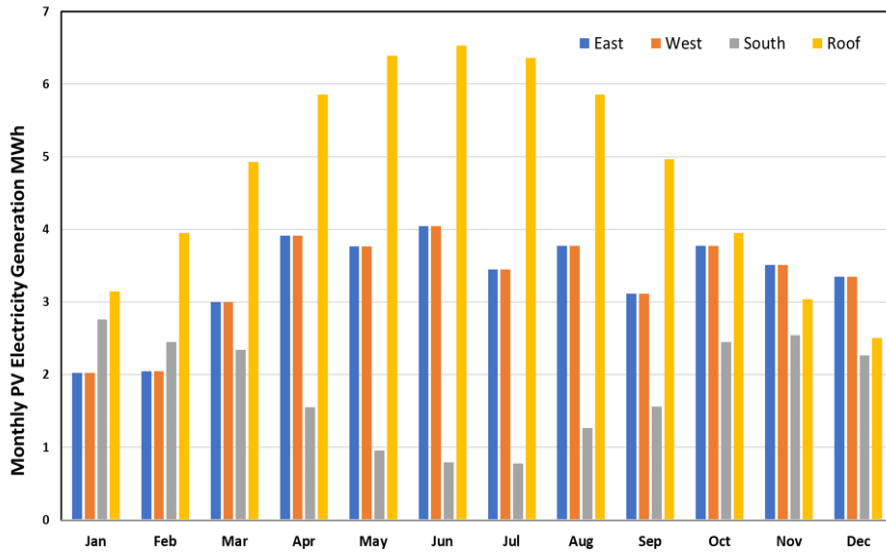


Figure 6. Monthly PV electrical generation for small facade compared to roof.

From Figure 6, the roof's PV installations generate more electricity during the entire year, as compared to the three studied vertical facades. Considering the facades, the east and west have more electrical power generation most of the year except January and February, compared to south façade. The entire facades have produced around 100 MW of electricity compared to 57 MW produced by the roof.

Lifecycle Cost Analysis

Table 4 shows that the LCCA relates to each studied configuration for 25 years studied period. From the table, the façade's installations require more cash to be paid compared to roof's installation.

Table 4. Life-cycle costs of each studied PV configuration based on 25 years period.

Studied Configuration	Initial Cost U.S. \$	O&M Cost U.S. \$ (Base Date)	UP _v Factor	LCC U.S \$
Roof	22800	1,140	22.076	47,966
Facade	25,840	1,292	22.076	54,362

Cash investment for the avoided conventional electrical power

Table 5 shows the outcomes of analyzing the performance of PV configuration from an economic point of view, considering the amount of electrical power that is annually lost due to degradation to be compensated by conventional power.

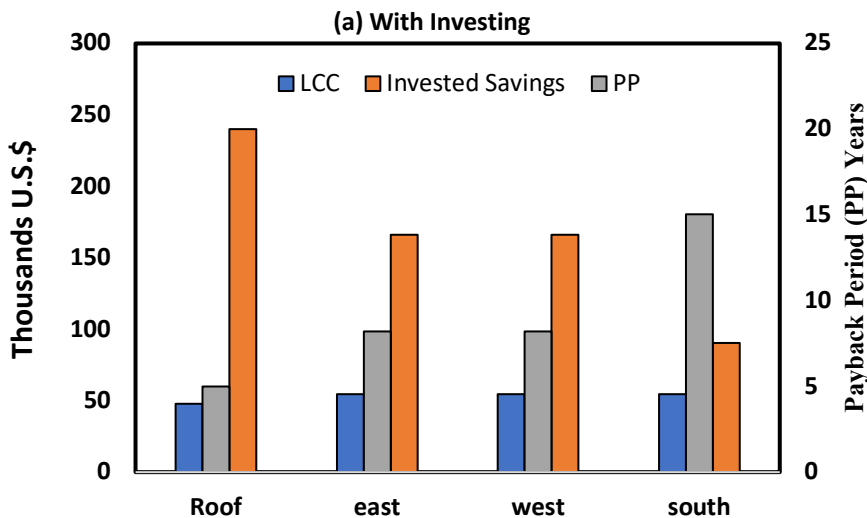
Table 5. 25 years PV net electricity generation, compensated conventional power and invested savings.

Installation Area		Net Power Generation (MWh)	Compensated Power (MWh)	Invested Savings US \$
Roof		1346	11.046	239,861
Vertical Facade	East	931.25	7.642	165,949
	South	507.95	4.168	90,517
	West	931.25	7.642	165,949

In Table 5, the roof has the largest PV electrical power generation followed by the façades facing east and west, and finally the south facing facade. In addition to the effect of installed PV area that allows for harvesting more solar irradiance to be converted to electricity, the directional orientations for vertical facades facing east and west seem to be an attractive choice for the buildings near the equator. However, the south facing facade directional can still produce a considerable amount of electricity in the studied period, looking at the potential of 25 years returns that result from the avoided conventional electricity.

Return On Investment

It was found that the roof has the best return on investment, followed by the east façade and west facade, and finally the south façade. The return on investment herein illustrates how many times the PV configuration can attain its total paid cost through its lifecycle. The roof scenario has the shortest break-even period to make the installation profitable with 5 years payback, followed by the east and west façades at 8.19 years payback each, and finally the south façade with 15.06 years. Relying on investing the annual savings is considered as an important factor to support installing PV modules on building’s facades, as shown in Figure 7.



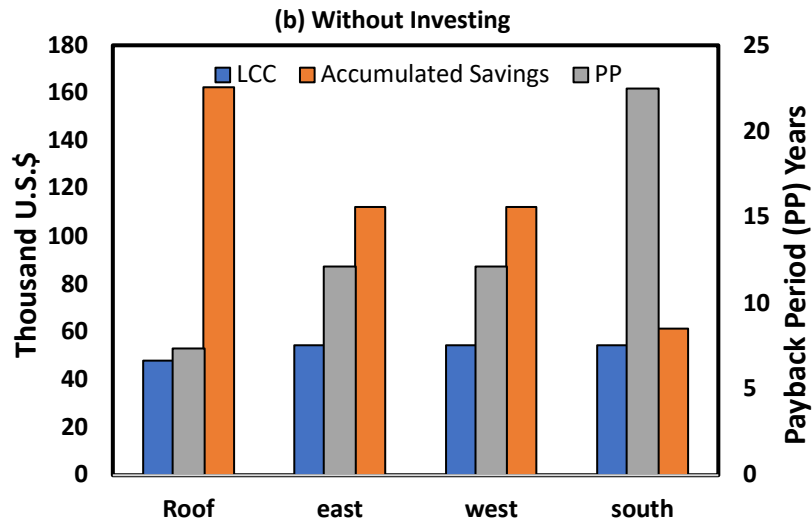


Figure 7. Economical evaluation for each PV configuration along 25 years period (a) with investing the annual returns (b) without investing the annual returns.

CONCLUSION

In this study, techno-economic analysis of different PV configurations attached to a residential building was evaluated. The vertical solar irradiances that are rarely recorded around the world have been calculated using a mathematical model. Geometry of potential buildings to attach PV modules plays a vital role in utilizing the surface area to maximize the harvesting of solar irradiance. The total generated electricity from the three promising façades (100 MW) is almost twice the roof's amount (57 MW). The building's orientation is a significant influencer that increases or decreases the building's solar power generation from an attached vertical PV system. The roof PV system has better power generation performance and subsequently shorter payback period compared to facades PV system but will not be sufficient for high demand in a harsh climate. The economic analysis proved that the vertical façades east, west, and south are feasible at payback years of around 8, 8, and 15, respectively, while the rooftop PV has the best economic feasibility by a payback period of 5 years. Payback period was calculated to demonstrate how effective is the installation of PV on vertical surfaces to generate electrical power compared to roof PV. Reinvesting the resulting cash from avoided conventional electricity is a feasible solution to shorten the payback period. The outcome of this work should encourage policymakers to incentivize the vertical surfaces to harvest solar energy.

ACKNOWLEDGMENT

This research is funded by the Public Authority for Applied Education and Training (PAAET) under project number TS-19-08. The authors take this opportunity to show their gratitude to PAAET for funding this work, which without it the work was not done.

REFERENCES

- Abdulrahman, A. 2020.** Executive director of Clenergy Mena company. Personal Communication (April, 2020).
- Ahmed, N., Alajmi, B., Abdelsalam, I., Marci, M., AlHajri, M.,** Advanced Maximum Power Point Tracker for PV Systems Under Dusty Weather Environments, *Transactions on Elec. And electronics Engineering, IEEJ*, vol. 17, no. 1, pp. 61- 71, January 2022.
- Central Bank of Kuwait (CBK) 2019.** The annual report of the central bank of Kuwait. Available from: <https://www.cbk.gov.kw/en/statistics-and-publication/publications/annual-reports>
- Fuller, S. & Petersen, S., 1995.** Life-cycle costing manual, US department of energy, NIST handbook 135.
- Gueymard, A. 2009.** Direct and indirect uncertainties in the prediction of tilted irradiance for solar engineering applications. *Sol. Energy* 2009, 83, 432–444.
- Hay, E. & Davies, A. 1978.** Calculation of the solar radiation incident on an inclined surface. In *Proceedings of the First Canadian Solar Radiation Data Workshop, Toronto, ON, Canada, 17–19 April 1978*; pp. 59–72.
- Hsieh, M., Chen, A., Tan, H., Lo, F. 2013.** Potential for installing photovoltaic systems on vertical and horizontal building surfaces in urban areas. *Solar Energy* 93, 312–321. Equation checked.
- Hofmann, M. & Seckmeyer, G. 2017.** A New Model for Estimating the Diffuse Fraction of Solar Irradiance for Photovoltaic System Simulations. *Energies* 2017, 10, 248.
- Hummon, M., Denholm, P., Margolis, R. 2013.** Impact of photovoltaic orientation on its relative economic value in wholesale energy markets. *Progress in Photovoltaic: Research and Applications* 21 (7), 1531–1540.
- IEA renewables 2019.** Market analysis and forecast from 2019 to 2024. Available from: <https://www.iea.org/reports/renewables-2019> (accessed May, 2020).
- IEA PVPS 2020.** Snapshot of global PV markets. Available from: <https://iea-pvps.org/snapshot-reports/snapshot-2020/> (accessed July, 2020).
- Jallal, M., Chabaa, S., Zeroual, A.** Half-hour global solar radiation forecasting based on static and dynamic multivariate neural networks. *Journal of Engineering Research*, Vol. 9, no. 2, pp. 203-217, June 2021.
- Karthick, A., Kalidasa, K., Kalaivani, L., Saravana, U. 2017.** Performance study of building integrated photovoltaic modules. *Advances in Building Energy Research*, DOI: 10.1080/17512549.2016.1275982.
- Khalil A. & Shaffie M. 2013.** Performance of statistical comparison models of solar energy on horizontal and inclined surface, *International Journal of Energy and Power* 2013; 2(1).
- Kumar, R. & Umanand, L. 2005.** Estimation of global radiation using clearness index model for sizing photovoltaic system. *Renew. Energy* 2005, 30, 2221–2233.
- Li, W., Lam, C., Lau, S. 2002.** A new approach for predicting vertical global solar irradiance. *Renewable Energy* 25, 591–606.
- Lee, M., Yoon, H., Kim, C., Shin, C. 2017.** Operational power performance of south-facing vertical BIPV window system applied in office building. *Solar Energy* 145, 66–77.
- Liu, B.; Jordan, R. 1961.** Daily insolation on surfaces tilted towards equator. *ASHRAE J.* 1961, 10, 526–541.
- Loutzenhiser, G., Manz, H., Felsmann, C., Strachan, A., Frank, T., Maxwell, M., 2007.** Empirical validation of models to compute solar irradiance on inclined surfaces for building energy simulation. *Solar Energy* 81, 254–267.
- Ministry of electricity and water (MEW) 2019.** Statistical yearbook

- Mohammad, A., Jaya, J., Al Hamadi, H., Alkandari, Dh.** The environmental cost and benefits analysis of different electricity options: a case study of Kuwait. *Journal of Engineering Research*, vol. 9, no. 2, pp. 308-319, June 2021.
- Mousavi Maleki, A., Hizam, H., Gomes, C.** 2017. Estimation of Hourly, Daily and Monthly Global Solar Radiation on Inclined Surfaces: Models Re-Visited. *Energies* 2017, 10, 134.
- Montoro, F., Vanbuggenhout, P., Ciesielska, J.** 2011. Building integrated photovoltaics: An overview of the existing products and their fields of application. Report prepared in the framework of the European funded project. SUNRISE, Saskatoon, Canada.
- Mubarak, R., Hofmann, M., Riechelmann, S., Seckmeyer, G.** 2017. Comparison of modelled and measured tilted solar irradiance for photovoltaic applications. *Energies* 10 (11), 1688.
- Muneer, T.** 1990. Solar radiation model for Europe. *Building services engineering research and technology* 11 (4), 153–163.
- Nejat, P., Jomehzadeh, F., Taheri, M.M., Gohari, M., Majid, M.Z.A.** 2015. A global review of energy consumption, CO₂ emissions and policy in the residential sector (with an overview of the top ten CO₂ emitting countries). *Renewable and Sustainable Energy Reviews* 43, 843-862.
- Notton, G., Poggi, P., Cristofari, C.** 2006. Predicting hourly solar irradiations on inclined surfaces based on the horizontal measurements: performances of the association of well-known mathematical models. *Energy Conversion Management* 47 (13), 1816–1829.
- Perez, R., Ineichen, P., Seals, R., Michalsky, J., Stewart, R.** 1990. Modeling daylight availability and irradiance components from direct and global irradiance. *Solar Energy* 44, 271–289.
- Reindel, T., Beckman, A., Duffie, A.** 1990. Evaluation of hourly tilted surface radiation models. *Sol. Energy* 1990, 45, 9–17.
- Şaylan, L., Şen, O., Toros, H., Arisoy, A.** 2002. Solar energy potential for heating and cooling systems in big cities of Turkey. *Energy Conversion and Management* 43 (14), 1829–1837.
- Shwehdi, M., Rajamohamed, S., Smadi, A., Bouzguenda, M., Alnaim, A., Fortea, S.** Energy savings approaches of buildings in hot-arid region, Saudi Arabia: case study. vol. 3, no. 1, pp. 127-136, March 2015.
- Spencer W.** 1975. Fourier series representation of the position of the sun. *Search* 1975;2(5):165–72.
- Tye, R., Haupt, E., Gilleland, E., Kalb, C., Jensen, T.** 2019. Assessing Evidence for Weather Regimes Governing Solar Power Generation in Kuwait. *Energies* 2019, 12, 4409.
- Yang, L., Yan, H., Lam, C.** 2014. Thermal comfort and building energy consumption implications—a review. *Applied Energy* 115, 164-173.
- University of Oregon. Solar Radiation Monitoring Laboratory** 2000. Available from: <http://solardat.uoregon.edu/> (Accessed July, 2020).